Assessment of air gap membrane distillation for milk concentration

Moejes, S. N., van Wonderen, G. J., Bitter, J. H., & van Boxtel, A. J. B.

Assessment of air gap membrane distillation for milk concentration

S.N. Moejes, G.J. van Wonderen, J.H. Bitter, A.J.B. van Boxtel*
Biobased Chemistry and Technology, Wageningen University
P.O. Box 17, 6700 AA, Wageningen, the Netherlands
E-mail: ton.vanboxtel@wur.nl

Abstract

Multi-effect evaporation is the state of the art for concentration of liquid food products to high solid content. Membrane technology with reverse-osmosis and membrane distillation offer an alternative. For the concentration of milk, a reverse osmosis and air-gap membrane distillation network was modelled and optimized. Fouling dynamics and scheduling are taken into account. Reverse osmosis is favourable until its maximum achievable concentration. Air gap membrane distillation is, despite the low operational temperatures, energy intensive for the concentration of milk. A large recirculation flow to keep sufficient cross flow has to be heated and cooled, and the costs for heating and cooling dominate the total costs for product concentration. Moreover, fouling increases the energy requirements. The optimal system for air gap membrane distillation has only one stage operating at a high concentration and relative low flux. Applying multiple stages reduces the investment costs due to smaller units, but the heating and cooling costs increase. Major opportunities to improve the performance of air gap membrane distillation for concentration of milk are: 1) increase the cold and hot side temperatures to their maximum acceptable values, 2) develop spacers that allow lower linear flow velocities in the system and thus lower recirculation rates, and 3) make use of available waste heat.

Keywords: Membrane distillation, milk, reverse osmosis, network optimization, process design

1 Introduction

Increasing need to reduce energy consumption and to use sustainable energy resources result in a demand for alternative product processing methods in the food industry. Traditional multi-stage evaporators used to concentrate food products are energy intensive, and require around 300 kJ per kg water removed [1]. This energy efficiency has increased in last decades due to the introduction of thermal and mechanical vapor recompression. Concentration by pressure driven membrane filtration, however, only requires 14 – 36 kJ per kg water removed [1]. The drawback of pressure driven membrane filtration is the achievable product concentration, which is limited due concentration polarization. For dairy products a maximum of 18% solids in the product stream is considered as economical feasible for reverse osmosis (RO) [2]. Membrane distillation (MD) is an emerging technology with the potential to concentrate to high solid contents. MD was developed as a desalination process in the 60's, and with the further development of suitable membranes in the 80's, the interest in this technology increased [3]. In more recent years MD gained attention for the concentration of food products, especially fruit juices and dairy products [4–7].

In MD, a porous hydrophobic membrane separates the feed and permeate phases and allows only water vapour to diffuse through the membrane. The driving force for mass transport is the partial vapour pressure difference between feed and permeate, which is related to the temperature difference over the membrane. As a result, the retention rate is very high, and high-quality water is produced as permeate. These advantages are the reason for the interest of MD for desalination and waste water treatment [3]. In contrast to other membrane processes, like reverse osmosis, ultrafiltration etc., MD is thermally driven instead of pressure driven. MD is therefore less affected by concentration polarisation [8]. For the concentration of milk a final solids concentration up to 45 – 50% is feasible by MD, which makes it a promising alternative for traditional evaporation [4,9,10].

Direct contact membrane distillation (DCMD) and air gap membrane distillation (AGMD) are most used for desalination and food applications. In DCMD the hot feed is separated by a hydrophobic membrane from a cold permeate stream. Water evaporates at the feed-membrane interface, passes through the membrane, and condensates at the membrane-permeate interface. In an AGMD configuration, on the other hand, water vapour from the feed passes through the membrane into an air gap, which on the other side is separated by a plate from a coolant at which the vapour condensates.

Advantage of AGMD compared to DCMD is the possibility of internal heat recovery, which results in a higher energy efficiency [11]. Therefore, AGMD has potential to compete with multi-effect evaporation and is considered in this study. A drawback of AGMD, on the other hand, is the lower flux compared to DCMD due to the smaller vapour pressure gradient [3]. Both systems operate at low temperatures, around 60°C, which makes MD processes interesting for heat sensitive products like fruit juices and dairy products. The thermal energy consumption is, however high compared to RO and modern multi-stage evaporators, with an energy consumption of 400 – 1300 kJ per kg water removed [1,12–16]. The advantage of MD is in the low operating temperatures, which allow the usage of low-quality heat, for example waste heat of other processes. Several studies suggested and investigated the usage of waste heat for operating the MD process [14,17–19]. In presence of abundant waste heat with temperatures of at least 40 – 70°C, MD might be an interesting alternative for traditional concentration methods like multi-stage evaporation.

For industrial applications MD will be applied in a network with RO network for pre-concentration. Both the RO and MD network consists of some concentration stages in series and in each stage a number of modules in parallel. Not only operational conditions, but also the configuration of a RO and MD network is crucial to guarantee a constant production, product quality, and minimum energy consumption. Several studies showed results on optimal membrane network designs, in which most focus on the synthesis of RO networks [20–24]. González-Bravo et al. [25] published the first results for the synthesis of a membrane distillation network for sea water desalination and dextrose syrup concentration. For seawater desalination the membrane distillation system had several stages with a different number of membrane units in parallel, while for dextrose syrup concentration a single stage system satisfied. At the start of this work it was not a priori clear what type of network configuration is most suitable for milk processing to high solids content. Another aspect that influences the network design for food products, like milk, is that fouling plays a dominant role due a gradual decline of mass and heat transfer over time. In pressure driven membrane application the flux decline can be compensated by an increase in operational pressure, but this option is not available for MD. Several authors investigated the effect of fouling on the operation of a single MD unit [8,9,26,27]. However, the effect of fouling on the design of a MD network is yet to be investigated.

Network design implies decision making at two levels. First, the main task of the network is to reach the aimed concentration. The number of stages in series and the concentration applied in each stage are decision variables to reach this aim. Low concentrations in the stages imply a high flux and a lower fouling rate and thus increasing the number of stages will be beneficial. However, a too high number of stages results in a larger membrane surface (and thus investments) and higher energy costs for fluid recirculation over a stage, and therefore there is an optimum in the number of stages. Secondly, fouling in the MD unit results in a serious decline of the product flow, which is not accepted if the product is directly further processed in a dryer or other installation. To remove fouling and to guarantee microbial safety, the installation must be cleaned at regular time intervals during which the production is interrupted. To keep a constant product flow and to minimize the interruptions of the operation, the parallel modules in each stage are operated in an operation-cleaning schedule. I.e. most modules are active in the operation, while others are being cleaned. This approach needs extra membrane surface per stage which raises the costs of the operation [28]. Also, due to the simultaneous stop and start of fouled and cleaned modules the product flow and concentration vary. The challenge is to design a schedule that limits the variation in product flow and concentration at low operational costs. To solve such complex problem a numerical simulation model is used. The model is based on mass and energy balances, and the best available experimental results from literature. Assumptions in the model are evaluated by variations in the main parameters and the role of process variables is investigated by a sensitivity analysis. With the sensitivity analysis the strengths, weaknesses, and potential of the system are qualified. Zhu et al. [22] approached this challenge for the design of a RO network and maintenance schedule for sea water desalination. The main differences with the current MD network design is that the RO flux was maintained constant over the operational period by increasing the pressure. Moreover, the operational window for cleaning was in the order of 50-100 days instead of 8-12 hours, which is needed for concentrating liquid food streams because of the stronger fouling rates and to prevent unacceptable growth of micro-organisms. This work presents a two-step approach whereby first the number of stages and membrane surface with the resulting concentrations in the succeeding RO and MD stages are obtained by mixed-integer non-linear optimization (MINLP). Secondly the scheduling problem is solved, finding the optimal number of parallel modules in each stage, by minimizing the total annual costs in combination with constrained variation of the product concentration and flow rate.

2 Process models

2.1 Membrane distillation

Unlike the extensive literature available for RO process models, MD only recently gained more interest especially as desalination technique. Most models are based on DCMD, however, because of the internal heat recovery the AGMD system is investigated in this study. The overall schematic representation of the AGMD module is shown in Figure 1. The membrane unit itself consists of a hot feed channel (hot side), hydrophobic membrane (dashed line), air gap, condensation plate (solid line), and the cooling channel (cold side). Furthermore, the module consists of a mixer, splitter, two heat exchangers, and pumps.

Fresh product feed is mixed with the recirculation flow, and the mixture is cooled to a fixed temperature before entering the cold side, in order to realize sufficient driving force over the membrane. On the other side the product is heated to a set temperature. The product flow from the heater enters the feed channel (hot side) of the membrane unit and water evaporates through the membrane, as depicted in Figure 1. The water vapour condenses at the wall of the air gap (solid line) due to the lower temperature in the cooling channel. The released heat of condensation results in an increase in product temperature in the cold side. The concentrated product from the membrane unit is partly recirculated to obtain sufficient crossflow in the membrane unit, which enhances heat transfer and reduces fouling. The other part of the concentrate is fed to next stage.

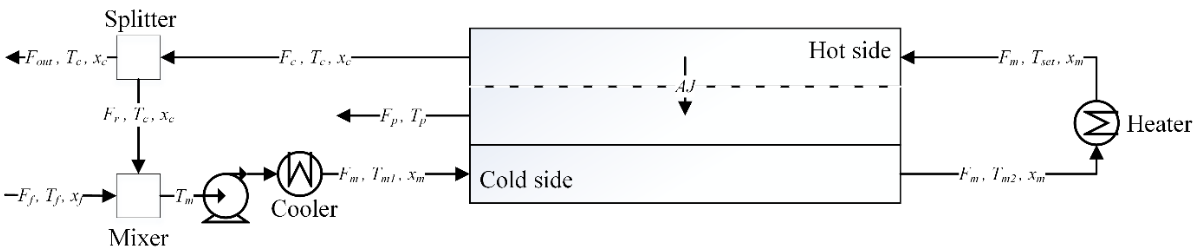

Figure 1. Schematic overview of a single AGMD module.

2.1.1 Mass transfer

The MD model is based on steady state mass and energy balances. These balances imply no loss of material and energy to the environment. The mass and energy balances over the MD module are:

$$F_m = F_f + F_r \tag{1}$$

$$F_m x_m = F_f x_f + F_r x_c \tag{2}$$

$$F_m c_{p,m} T_m = F_f c_{p,f} T_f + F_r c_{p,r} T_c \tag{3}$$

$$F_r = N_{MD} A_{channel} v_{lin} \rho \tag{4}$$

where F is the mass flowrate and x the concentration of solids, c_p the heat capacity of the flow, T the temperature of the flow, and subscripts m, f, r are denoting mix, feed, and recirculation loop respectively. The recirculation flow (F_r) is dependent on the linear flow velocity (v_{lin}), the number of parallel membrane units (N_{MD}), the cross-sectional area of the membrane channel ($A_{channel}$), and the density of the milk (ρ). The mass balance over the membrane unit itself is given by:

$$F_m x_m = F_c x_c \tag{5}$$

$$F_f = F_{out} + F_p = F_{out} + JA \tag{6}$$

where J is the water flux through the membrane and A the membrane surface area. According to Hausmann et al. [29] the retention rate of MD for dairy components ranges from 99 to 100%, therefore no component losses via the permeate are assumed in this work.

The water flux is based on the difference between the vapour pressures at the feed (P_f) and the condensing layer (P_{cl}), and the overall resistance. The vapour pressure is calculated based on the saturated vapour pressure, temperature and mole fraction of water.

$$J = \frac{P_f - P_{cl}}{R_{fl} + R_{mem} + R_{ag}} \tag{7}$$

The overall resistance consists of the resistance of the fouling layer (R_{fl}), the membrane (R_{mem}), and the air gap (R_{ag}). Figure 2 gives an overview of the different layers. The fouling resistance is discussed in section 2.1.3. Membrane resistance is described by the combined Knudsen and molecular diffusion model. The membrane and air gap resistance are based on the work of Drioli et al. [30] and Hausmann [10]. The width of the air gap decreases with the increase of the condensing layer towards the outlet of the module, however, in this work the condensing layer is assumed to be equal over the whole length of the module.

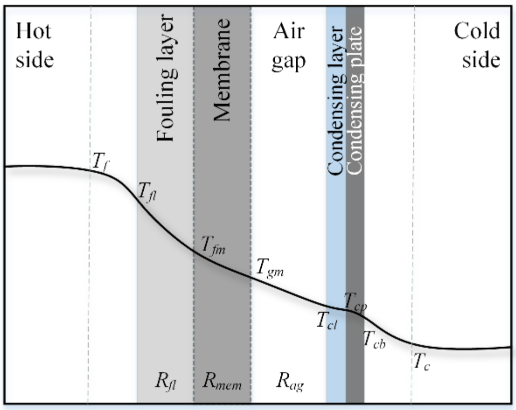

Figure 2. Schematic overview of the different resistance layers and temperature profile in the AGMD module.

General characteristics of milk like viscosity, density and specific heat capacity are influenced by the concentration and temperature. Viscosity estimations are based on Fernández-Martín [31], equations for density and specific heat capacity are both taken from Choi et al. [32].

2.1.2 Heat transfer

The vapour pressure, and thus the flux, relies on the temperature (T_{fm}) at the membrane surface and condensing layer (T_{cl}) interface. The interfacial temperatures are calculated based on the overall heat transfer. Assuming the MD module operates at steady state without heat losses to the surroundings, the heat transfer equals:

$$\Delta Q = h_{bf}(T_f - T_{fl}) = \frac{\lambda_{fl}}{\delta_{fl}}(T_{fl} - T_{fm}) = J\Delta H_v + \frac{\lambda_{mem}}{\delta_{mem}}(T_{fm} - T_{gm}) = \frac{\lambda_{ag}}{\delta_{ag}}(T_{gm} - T_{cl}) + J\Delta H_v = \frac{\lambda_{cl}}{\delta_{cl}}(T_{cl} - T_{cp}) = \frac{\lambda_{cp}}{\delta_{cp}}(T_{cp} - T_{cb}) \quad (8)$$

in which ΔQ is the amount of transferred heat, T the temperatures at different locations, h is the heat transfer coefficient, δ the thickness, λ the conductivity of the specific layer, and ΔH_v the heat of evaporation. The different layers are visualised in Figure 2. The heat transfer coefficient of the membrane is given in Equation (9). Parameters and variables used are listed in Table A.1.

$$h_m = \frac{\left(\frac{\epsilon_m}{k_g} + \frac{1-\epsilon_m}{k_m}\right)^{-1}}{\delta_m} \quad (9)$$

in which ϵ_m is the membrane porosity, k_m is the membrane material conductivity, and k_g is the thermal conductivity of air in the membrane pores.

Since both the flux and the interfacial temperatures depend on each other, an iterative model is used to calculate the interfacial temperatures. The vapour flux is from the feed channel to the air gap. The energy required in the heater (Q_{heat}) and the energy transferred in the cooler (Q_{cool}) is given by the following energy balances.

$$Q_{heat} = F_m c_{p,m}(T_{set} - T_{m2}) \quad (10)$$

$$Q_{cool} = F_m c_{p,m}(T_{m1} - T_m) \quad (11)$$

in which T_{set} is the set operating temperature of the membrane module at the inlet of the hot side, T_m is the temperature after the mixer, and T_{m1} and T_{m2} are the temperature of the product flow at the in- and outlet of the cold side, respectively. T_{set} and T_{m1} are controlling parameters and fixed in the operational conditions.

Electrical energy, required for the pumps, is based on the size of the stream (F_m), the pressure drop over the system (ΔP_{drop}), and the energy efficiency of the pump (η_{pump}).

$$E_{pump} = \frac{F_m \Delta P_{drop}}{\eta_{pump}\rho} \quad (12)$$

2.1.3 Fouling model MD

Deposition of product components on the membrane over time results in a gradual increase of resistance for mass and energy transfer over the membrane. According to Hausmann et al. [26] the fouling mechanism of skim milk in membrane distillation relies on the interaction between milk proteins, caseins, and salts, which form a gel like layer. However, Tijing et al. [8] pointed out, that the mechanism of fouling in membrane distillation is not yet extensively studied and as well understood as for pressure driven membrane processes. As fouling has a major impact on flux decline, and thus process performance, it is of importance to be included in process design and simulation.

A homogeneous fouling layer on top of the membrane is formed during the concentration of skim milk by MD, and to a lesser extent by adhesion inside the pores [26]. The formation of the fouling resistance can, therefore, be described by a cake filtration or gel layer model [33]. The linear relationship between the fouling resistance and the thickness of the fouling layer results in the following equation [34].

$$\frac{dR_{fl}}{dt} = \frac{\epsilon_{fl} c_b}{\rho} J - \frac{\epsilon_{fl} c_b k_f}{\rho} ln\left(\frac{c_{fl}}{c_b}\right) \tag{13}$$

in which ϵ_{fl} is a constant for the resistance per unit of fouling layer thickness, c_b and c_{fl} are the concentration in the bulk and the fouling layer respectively, k_f is a mass transfer coefficient, and ρ the density. As we aim to study the effects of different levels of fouling on the organisation of the membrane system, and not to reveal the mechanism, the parameters in equation (13) are lumped, as suggested by van Boxtel et al. [35]. This results in the following semi-empirical equation:

$$\frac{dR_{fl}}{dt} = aJc_b - b \tag{14}$$

in which a and b are the lumped parameters and must be estimated from experimental data. Due to the lack of experimental data for the concentration of dairy or food products by AGMD, data for the concentration of skimmed milk by DCMD from Hausmann et all [10] was used to estimate these constants. Data validation is listed in Appendix A.2. The thickness of the fouling layer (δ_{fl}) is estimated by a linear relationship to the fouling resistance [35].

$$\delta_{fl} = \frac{R_{fl}(t)}{\epsilon_{fl}} \tag{15}$$

2.2 *Reverse osmosis*

The RO system (see Figure 3) consists of a high-pressure pump to pressurize the incoming feed to the desired operating pressure. Inside the apparatus the concentrate is to a large extend recirculated and mixed with the incoming feed to achieve high concentration factors and to have sufficient flow rate to prevent concentration polarization. After mixing the feed and recirculation flow a booster pump will provide the extra pressure that was lost over the module and to ensure operating pressure is maintained. After passing the module the concentrate is split into a recycle flow and a concentrate flow which is fed to the next stage.

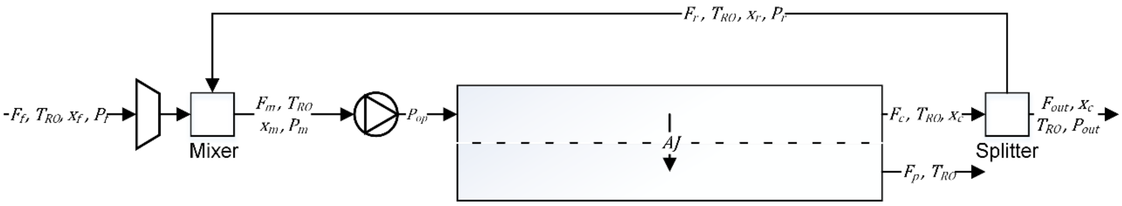

Figure 3. Schematic overview of the reverse osmosis modules.

2.2.1 Mass and heat transfer

The mathematical framework of the described system is based on the descriptions given in [22,36]. It is assumed that the feed flow (F_f) and the recirculation flow (F_r) are constant, and the recirculation flow is a fixed fraction (r_{RO}) of the feed flow.

$$F_m = F_f + F_r \quad (16)$$

$$F_m x_m = F_f x_f + F_r x_c \quad (17)$$

$$F_r = \frac{F_f}{1/r_{RO} - 1} \quad (18)$$

$$F_p = AJ = F_f - F_{out} \quad (19)$$

where A is the membrane area and J is the flux. The flux in a RO unit is based on the pressure difference over the membrane and the overall resistance (R_{ov}). In this study it is assumed that there are no losses through the membrane.

$$J = \frac{P_{op} - P_p - \pi}{R_{ov}} \quad (20)$$

where P_{op} ,P_p and π are the feed pressure, the pressure at permeate side, and the osmotic pressure respectively. To guarantee a constant flux over time, the operating pressure is increased from 40 MPa to a maximum of 70 MPa to compensate for extra resistance due to fouling [20,22]. The osmotic pressure (π) is calculated as follows:

$$\pi = x_f R_{gas}(T_{RO} + 273) \quad (21)$$

where x_f is the molar concentration of the feed, R_{gas} the gas constant, and T the absolute temperature.

R_{ov} is the overall resistance consisting of the intrinsic membrane resistance (R_{mem}), the start-up resistance (R_p) and the fouling resistance (R_{fl}).

$$R_{ov} = R_{mem} + R_p + R_{fl} \quad (22)$$

$$R_{mem} = \frac{1}{D_w \gamma} \quad (23)$$

where D_w is the water permeability, and γ is a variable encompassing the membrane characteristics derived from Zhu [22].

The energy requirements for a RO unit are based on the electrical energy used by the pumps. The energy usage of the high-pressure pump is:

$$E_{hp,pump} = \frac{F}{\eta_{hp}\rho}(P_{op} - P_{in}) \quad (24)$$

2.2.2 Fouling model RO

The used fouling model for RO is the same as for MD (Equation (13)). The vapour pressure difference used in the MD model as driving force is, however, replaced by the pressure difference over the membrane ($\Delta P = P_{op} - P_p - \pi$). The constants in the model are estimated by fitting the model to published data [35,37]. The parameters used for the RO model are given in Table 1.

2.3 Overview of model assumptions

The presented models are based on mass and energy balances, and no loss of energy and material was assumed. For the flux in the MD system standard heat transfer equations are applied. Hausmann et al. presented the equations for DCMD [10] and a MD system with integrated heat exchange [17]. The equations for the AGMD correspond to those of the MD system with integrated heat exchange. The performance of the system calculated by the model depends on the applied constants in the model. Table 1 presents the applied constants and shows that the major part of these constants are derived from literature, or from specifications of membrane suppliers. Four constants from the table are less certain (membrane thickness, condensation layer thickness, thermal conductivity membrane, and membrane resistance) and in a sensitivity analysis the effect of these parameters is evaluated by changing the values ±20%. For the RO model all constants are well defined by literature or equipment suppliers, and therefore assumed to give an accurate prediction of the systems performance.

The flux decline due to membrane fouling can be caused by several mechanisms. Although a model proposed for cheese whey fouling on RO was used for MD, a realistic fouling pattern was simulated by fitting the model to experimental data published by Hausmann et al. [10]. The same model was also fitted to experimental data of RO [35,37]. In line with current practice the potential flux decline in RO was compensated by an increase of the operational pressure. Variations in the fouling behaviour in MD are evaluated by a sensitivity analysis of the fouling parameters.

Table 1. Membrane specific process parameters

Membrane specifications	Value	Reference
RO spiral wound		
Water permeability (kg s^{-1} N)	3×10^{-10}	[22]
Fixed recirculation fraction in RO module	0.95	equipment data
Membrane resistance (Pa s m^{-1})	1.27×10^{12}	[35,37]
Start-up resistance (Pa s m^{-1})	2.13×10^{10}	[35,37]
MD flat sheets		
Air gap width (m)	1×10^{-3}	[11]
Condensation layer thickness (m)	1×10^{-4}	10% of air gap
Membrane thickness (m)	6×10^{-5}	equipment data
Condensation plate thickness (m)	6×10^{-5}	equipment data
Cross sectional area channel (m2)	1.5×10^{-3}	equipment data
Membrane porosity (-)	0.8	[11]
Resistance per unit of fouling layer (Pa s m^{-1})	8×10^{-11}	[35]
Membrane resistance (Pa s m^{-1})	1.6×10^{5}	[10]
Thermal conductivity condensation layer (W m^{-1} K^{-1})	0.58	[38]
Thermal conductivity condensation plate (W m^{-1} K^{-1})	24	[38]
Thermal conductivity membrane (W m^{-1} K^{-1})	1.2	[11]
Thermal conductivity fouling layer (W m^{-1} K^{-1})	0.23	[39]
Thermal conductivity air (W m^{-1} K^{-1})	0.027	[38]
Latent heat of evaporation (kJ kg^{-1})	2257	[38]
Gas constant (J K^{-1} mol^{-1})	8.314	[38]

3 Approach and problem formulation

The combined model equations of the membrane system (Eq. 1-22) are non-linear, and the number of units are integer variables. Therefore, the optimization of the network configuration of RO and MD is a mixed integer non-linear problem (MINLP). A downside of these problems is the complexity and the required computational time. The optimization problem is, therefore, split into two parts: 1) the estimation of the optimal number of RO and MD modules in series (*N*) and their respective total membrane surfaces, and 2) the scheduling problem where the optimal number of parallel units (*M*) and scheduling strategy is derived. Figure 4 gives an example of the possible membrane network.

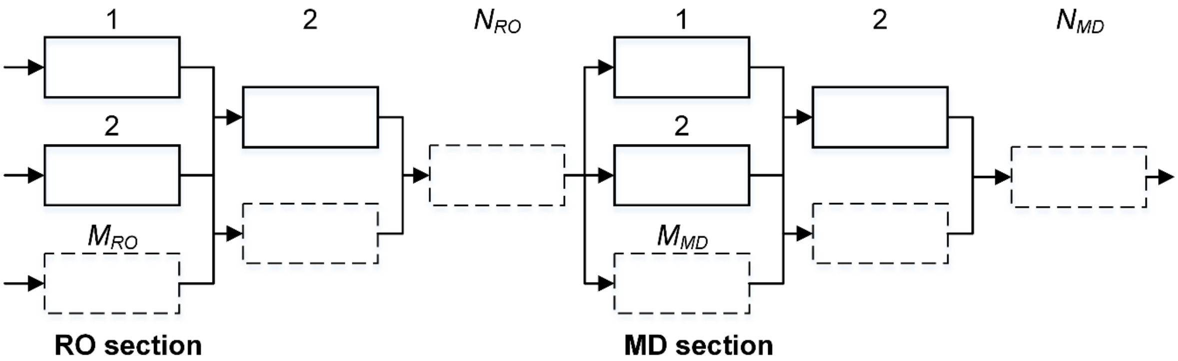

Figure 4. Schematic representation of a RO and MD network. N_{RO}, and N_{MD} the number of membrane stages in series for RO and MD, and M_{RO}, and M_{MD} the number of membrane unit in parallel for each RO and MD stage.

3.1 Stage optimization

Each potential stage is considered as one large membrane module for which the total surface is estimated. The decision variable is the membrane surface in each stage, which results in a specific product concentration after each stage. The objective is to design a network with the lowest investment and operational costs that realizes a given final product concentration for a given feed rate. The objective function is formulated as:

$$min \left(\sum_{n=1}^{N_{RO}} C_{RO,inv}^{n} + \sum_{n=1}^{N_{RO}} C_{RO,op}^{n} + \sum_{n=1}^{N_{MD}} C_{MD,inv}^{n} + \sum_{n=1}^{N_{MD}} C_{MD,op}^{n} \right) \tag{25}$$

s.t. $c_{goal} \leq \bar{c}_{out,(n=N)}$

$Equations\ 1 - 23$

where C_{inv} are the investment costs and C_{op} are the operational costs for each stage n for the total number of stages N for both RO and MD. The operational conditions and process boundaries are listed in Table A.2.

The investment costs for RO consist of the equipment costs of the pumps, and the RO module which consists of the module costs ($C_{RO,mod}$) and the membrane costs ($C_{RO,mem}$), which both are linearly related to the surface membrane surface (A). The installation costs are covered by a Lang factor (L_f). The total costs are annualised by the life time of the equipment (LF) and the life time of the membranes LF_m. Subsequently all costs are expressed in euro per m^3 water removed.

$$C_{RO,inv} = \frac{\left(\frac{C_{pump,n}}{LF_{pump}} + \frac{A_n C_{RO,mod}}{LF_{mod}}\right) L_f + \frac{A_n C_{RO,mem}}{LF_{mem}}}{F_{p,a}} \tag{26}$$

The operational costs for RO contain the electrical cost for the pumps and the cleaning costs, both are annualized. Cleaning costs depend on the membrane surface (A_n) and the total cleaning time (t_{clean}).

$$C_{RO,op} = \frac{(E_{electric,n} C_e t_a + C_{clean} A_n)}{F_{p,a}} \tag{27}$$

Furthermore, the concentration of the last stage ($\bar{c}_{out}$) should not be lower than the set concentration (c_{goal}). The final concentration for RO is a decision variable but is limited to a final concentration of 18%. Output parameters (flow, concentration, and temperature) of the last stage of RO are the input parameters of the first stage of the MD section.

The MD investment costs and operational costs are formulated similar as for RO but contain additional components. In addition, the investment costs include the heat exchangers for heating and cooling. The membrane costs for MD are calculated in the same way as for RO. The operational costs also include the heating and cooling for every MD module, which results in the following equations.

$$C_{MD,inv} = \frac{\left(\frac{C_{pump,n} + C_{heater,n} + C_{cooler,n} + A_n C_{MD,mod}}{LF_{mod}}\right) L_f + \frac{A_n C_{MD,mem}}{LF_{mem}}}{F_{p,a}} \tag{28}$$

$$C_{MD,op} = \frac{(E_{electric,n} C_e + E_{heat,n} C_{heat} + E_{cool,n} C_{cool}) t_a + C_{clean} A_{tot} t_{clean}}{F_{p,a}} \tag{29}$$

MD is proposed as an alternative for multi-stage evaporation of milk, therefore, the final concentration of the last MD stage is fixed at 50% total solids. The resulting configuration is used as input for the scheduling optimization. Figure 5 illustrates the total optimization procedure, whereby Figure 5 part I represents the stage optimization. To solve the series problem the fmincon function of MATLAB R2017b with the interior point method algorithm was used.

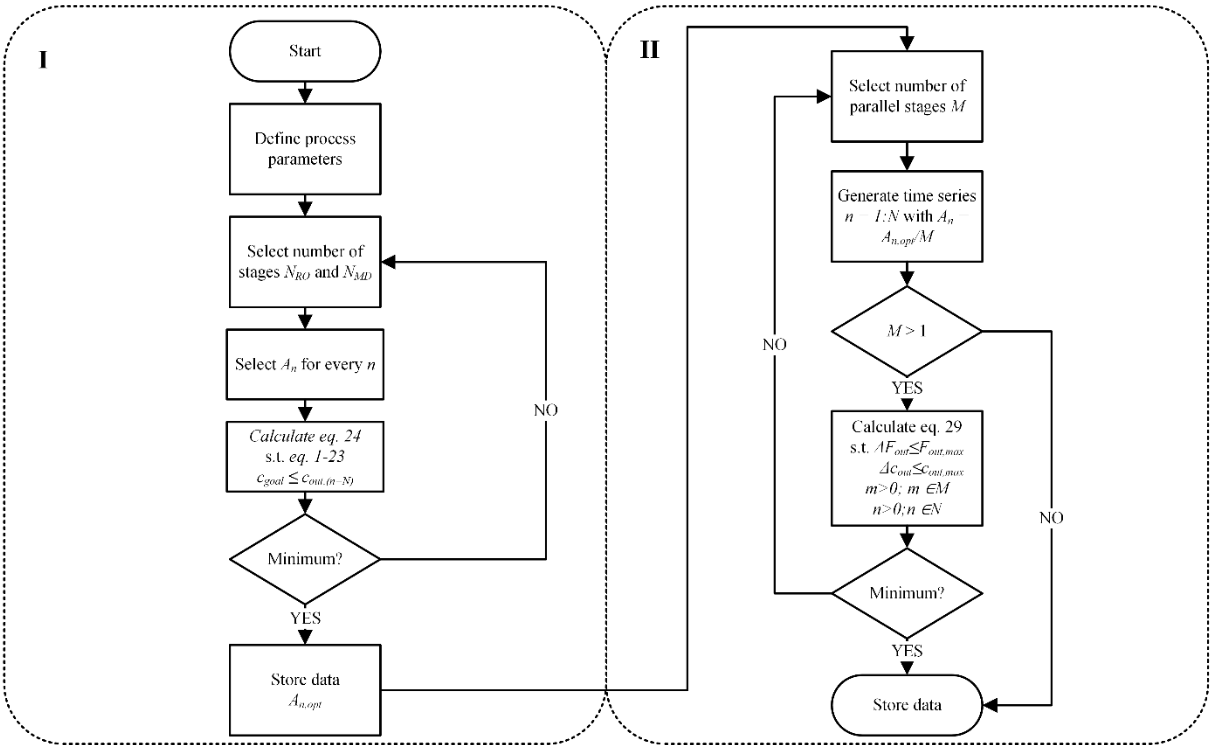

Figure 5. Solution strategy for an optimal membrane design. With I) the selection of the optimal number and area of RO and MD units in series, and II) the strategy for the scheduling problem and the selection of number of parallel units.

3.2 Scheduling strategy

The optimal scheduling strategy is based on the number of parallel units (M) and aims to guarantee a continuous production while minimizing the costs. For the economical evaluation of the different configurations the total costs are minimized. These consists of the annualized investment costs (C_{inv}) and the annual operational costs (C_{op}) of both the RO (C_{RO}) and the MD section (C_{md}). The operational conditions and process boundaries are listed in Table A.1.

$$\min\left(\sum_{n=1}^{N_{RO}}\sum_{m=1}^{M_{RO}} C_{RO,inv}^{n,m} + \sum_{n=1}^{N_{RO}}\sum_{m=1}^{M_{RO}} C_{RO,op}^{n,m} + \sum_{n=1}^{N_{MD}}\sum_{m=1}^{M_{MD}} C_{md,inv}^{n,m} + \sum_{n=1}^{N_{MD}}\sum_{m=1}^{M_{MD}} C_{md,op}^{n,m}\right) \quad (30)$$

$$\begin{aligned} \text{s.t. } & \Delta F_{out}^{n,m} \leq \Delta F_{out,max} \\ & \Delta c_{out,nm}^{nm} \leq \Delta c_{out,max} \\ & m > 0;\ m \in M \\ & n > 0;\ n \in N \\ & Equations\ 1-23 \end{aligned}$$

The next step in milk processing is spray drying, a unit operation that requires a constant feed rate and product concentration. Therefore, fluctuations in flow rate and concentrations have to be limited. For the RO section the deviation in outflow of every stage ($\Delta F_{out,max}$) may not be larger than 10%. In the MD section the final concentration will fluctuate due to the flux decline over time, therefore, the variation in final concentration ($\Delta c_{out,max}$) is restricted to 1.5% over the whole production period. These were set as constraints in the minimization problem.

The investments costs consist of the cost of the membrane units, pumps and heat exchangers, which depends on the number of stages (N) and parallel units (M). The investment costs are annualized and corrected with a Lang factor (L_f) [40].

$$C_{md,inv} = \frac{\dfrac{\left(C_{pump,mn} + C_{heater,mn} + C_{cooler,mn} + A_{mn}C_{md,mod}\right)}{LF_{mod}} L_f + \dfrac{A_n C_{md,mem}}{LF_{mem}}}{F_{p,a}} \quad (31)$$

$$C_{RO,inv} = \frac{\left(\frac{\left(C_{pump,mn} + C_{md,mn} + A_{mn}C_{RO,mod}\right)}{LF_{mod}}L_f + \frac{A_{mn}C_{RO,mem}}{LF_{mem}}\right)}{F_{p,a}} \tag{32}$$

The costs for the membrane distillation unit (C_{md}) consists of the membrane module (C_{mod}) and the membrane (C_{mem}) itself which all depend on the membrane area (A). The investment costs for the RO section are calculated in the same way, only without the heater.

The operational costs are based on the costs for electricity, heating, cooling, and cleaning. The cleaning consists of both thermal energy (E_{clean}) for cleaning and the material costs (C_{clean}), and depend on the number of operational hours (t_{op}).

$$C_{MD,op} = \frac{\left(E_{electric,mn}C_e + E_{clean,mn}C_{heat} + E_{heat,mn}C_{heat} + E_{cold,mn}C_{cold}\right)t_{op} + C_{clean}A_{tot}t_{clean}}{F_{p,a}} \tag{33}$$

$$C_{RO,op} = \frac{\left(E_{electric,mn}C_e + E_{clean,mn}C_{heat}\right)t_{op} + C_{clean}A_{tot}t_{clean}}{F_{p,a}} \tag{34}$$

Other auxiliary equipment, maintenance, and labour costs are not considered. To solve the scheduling problem the pattern search method of MATLAB R2017b was used.

For estimation of the number of parallel modules and the best scheduling strategy it was assumed that all modules have fixed production cycles of 7 hours followed by a 1 hour cleaning cycle, this to guarantee food safety. Furthermore, the membranes will operate at the same initial performance after every cleaning cycle, so fluxes are fully restored. Additionally, it was assumed that the modules operate after cleaning immediately at steady-state, and the operating conditions of each parallel unit in the same stage are identical. Figure 5 part II shows the solution strategy. Data generated in the series configuration section is used as input for generating the time series which are the input for the scheduling problem. All cost parameters are listed in Table A.2. The effect of the usage of waste heat on the total costs are evaluated in additional optimizations, as well as the effect of the operational conditions on the total performance.

4 Results and discussion

4.1 Process design

The optimal process configuration to concentrate milk from 0.09 kg kg^{-1} to 0.5 kg kg^{-1} solids is by a two-stage RO section and a single-stage MD section. The optimal process configurations for the RO and MD section are shown in Figure 6, and details are displayed in Table 2. RO proved to be more cost efficient compared to MD. Milk is, therefore, concentrated by RO to the upper boundary of 0.18 kg kg^{-1} solids. A two-stage RO configuration is optimal for this case, which both consist of six parallel units. The energy consumption of the RO section resulted in 19 kJ per kg water removed, which is in line with reported values in literature [1].

Table 2. Results for the optimal total system with specifications of the configuration and performance of the RO and MD sections. RO concentrates milk from 9% to 18% dry matter and MD from 18 to 50% dry matter.

		Total system	RO section	MD section
Feed	tonne h^{-1}	25	25	12.5
Total membrane area	m^2	5300	1416	3884
Number of series	-	2 – 1	2	1
Number of parallel units in subsequent stages	-	6 – 6 – 4	6 - 6	4
Heating costs	€ m^{-3}	3.2	-	8.3
Cooling costs	€ m^{-3}	2.3	-	6.0
Electrical costs	€ m^{-3}	1.1	0.6	1.7
Equipment costs	€ m^{-3}	0.9	0.2	2.1
Cleaning costs	€ m^{-3}	0.5	0.2	1.0
Total costs	€ m^{-3}	8.1	1.0	19.1

Figure 6 shows the configuration for the RO and MD stages with operational conditions. In the figure the optimal MD configuration with one stage is given. Alternative, sub-optimal, MD configurations with operational conditions are given in appendix A.3.

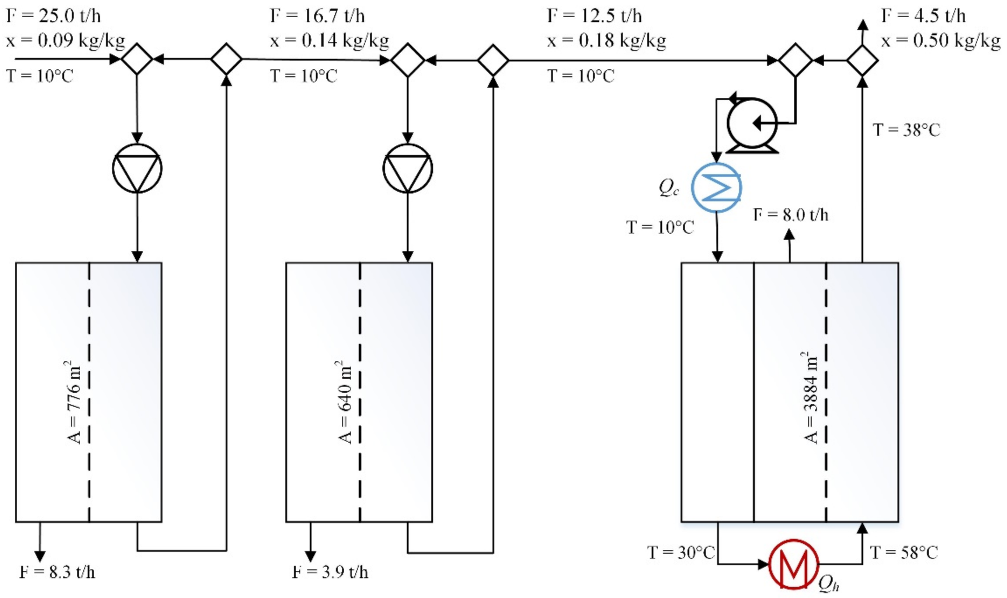

Figure 6. Optimal process configurations for the combined RO (first 2 stages) and MD (3rd stage) system, including average flows, concentrations, and temperatures.

The costs for the optimal RO and MD configurations and the combination of the two (total system) are listed in Table 2. To reach the end concentration of 0.5 kg kg^{-1} solids a single stage MD turned out to be best in terms of costs. Although the result corresponds to the work of González-Bravo et al. [25] for dextrose syrup concentration the result is counter-intuitive as the single stage AGMD system operates at a high concentration with a low flux and stronger fouling compared to a multi-stage system. No advantage is taken from the higher fluxes and lower fouling rate in the first stages of a multi-stage system (see Figure 7 for a specification of the fluxes in subsequent stages). The required membrane area and thus investment costs of this single-stage system are therefore higher than that of a multi-stage MD system. Details of multi-stage MD systems are listed in Appendix A.3. The membrane area proved, however, not to be the main cost driver, but the heating and cooling costs are (Table 2). Due to the required recirculation in each of the subsequent stages, to keep sufficient cross flow along the membrane surface, the increase of heating and cooling costs is larger than the reduction of the capital costs. Ignoring heating and cooling costs in the simulations resulted in a multi-stage system with low investment costs for membranes (like seawater desalination). Moreover, the flux decline over time plays an important role in the costs. Due to the flux decline the internal heat recovery decreases and as a consequence more heating and cooling is required in the recirculation loop during operation. Altogether, the costs of a two-stage system are 16% above those of a single-stage MD system.

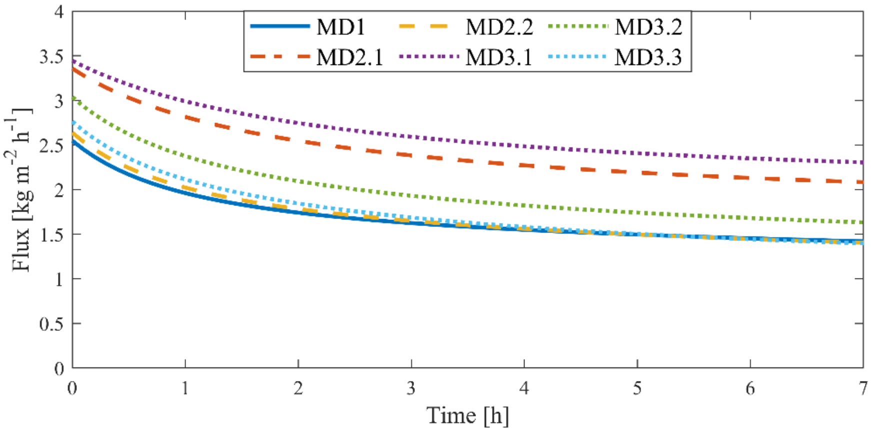

Figure 7. Flux profile over time in the different MD stages. Single stage: MD1, a two-stage: MD2 and a three-stage system: MD3.

Concentration of food products like milk by MD has the advantage of reaching a high final concentration by using a membrane system. However, the energy consumption is high compared to concentration by RO. For milk concentration, besides heating also cooling of the recirculation loop is necessary in order to maintain the driving force. The energy required for a single stage system is 2.6 MJ for heating and 2.5 MJ per kilogram water removed for cooling, which is much higher compared to previously reported values for MD on desalination [12–16] and traditional multi-stage evaporator systems. Cooling is not required for desalination, as the permeate is the aimed product, and not the concentrate which is aimed for food products like milk. Reported costs values for desalination range between 0.3 and 5.1 euro per m^3 water removed [18,25,41]. For milk the costs for MD are estimated at nearly 20 euro per m^3 water removed. However, when combining MD and RO the total costs are 8.1 euro per m^3 water removed. This is still higher when compared to reported desalination values but does include the effect of fouling and the additional energy costs caused by the high recirculation and for cooling.

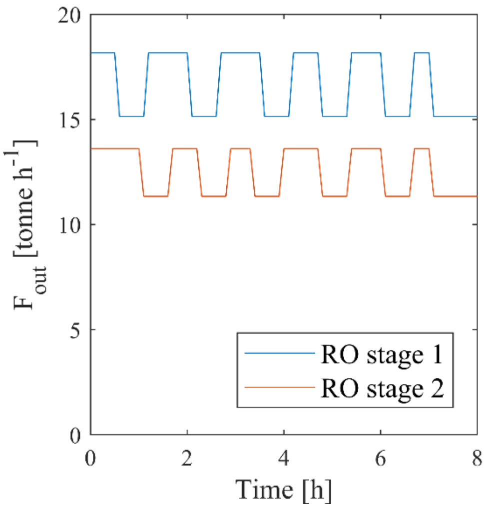

Figure 8. Effect of scheduling on the product out flow for a two stage RO system with 6 parallel units in each stage. At the high values all modules are in operation, at the low values one module is in the cleaning mode.

In each stage a number of parallel membrane modules are operational. Each membrane unit is operational for 7 hours, followed by a rinsing and cleaning period of one hour. With these intervals the flux and concentration would be constant if in each stage consisted of 8 parallel modules. If less modules prove to be optimal variation in outflow (RO and MD) and concentration (MD) will result.

In order to minimize fluctuation in flow to the next module, scheduling for the RO part is based on keeping the milk outflow within fixed boundaries of ±10%. The flux, and thus milk concentration, is kept constant by increasing the operating pressure over time. Allowing a flow variation of ±10% from the RO system, the optimization resulted in 6 parallel modules in each stage. The use of 6 parallel modules in each stage implies that over the full scheduling period, during short times all parallel modules are operational, which causes the flow variations in Figure 8.

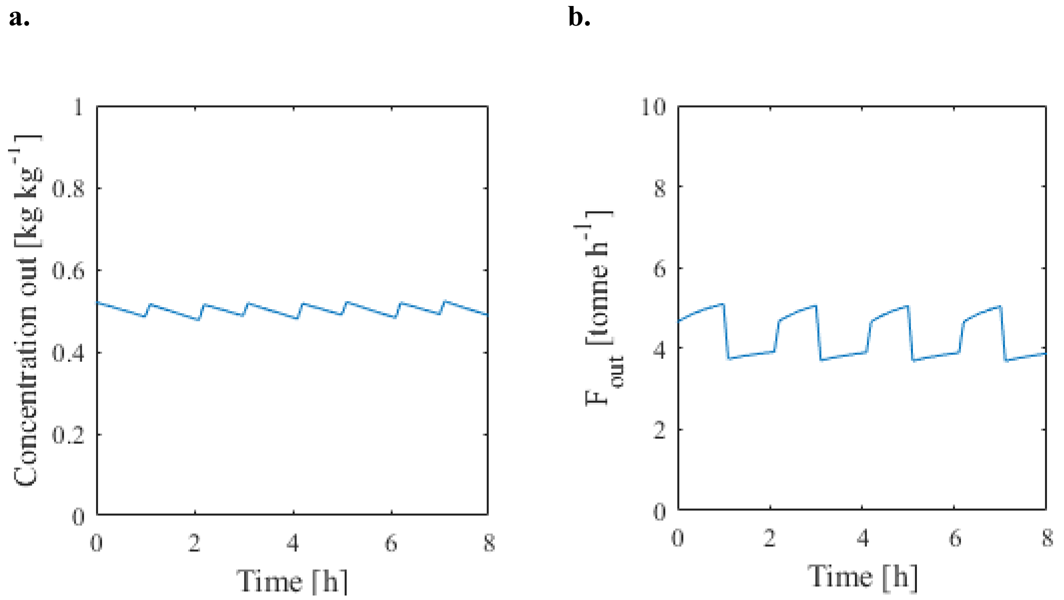

Figure 9. Effect of scheduling on MD for the product concentration (a) and product flow (b) of 4 parallel units in a one-stage system. The gradual decline of concentration and increase of flow is result of the fouling.

For MD, 4 parallel modules for the one-stage system are enough to keep the final concentration within the pre-defined operational boundaries (maximum fluctuation of 1.5% for the final concentration). In this scheduling system all 4 parallel units are used during 1.3 hours, then one unit is in the cleaning mode (Figure 9). These events cause the step variations in the graphs for concentration and flow. Moreover, during the operation of the membrane units, the flux declines gradually. As a result, the product outflow increases over time as the permeate flow decreases as a result of the flux decline until the next cleaning cycle. These gradual variations were absent for RO, where the flux reduction due to fouling is compensated by increasing the operational pressure.

4.2 Effect of fouling rate

Previous studies on MD featured a significantly lower fouling rate [40,42], or did not include the fouling dynamics at all [25]. Fouling, however, plays an important role in milk concentration by membrane processes. Although the fouling dynamics used in this study is based on assumptions, it gives an insight on the effect of fouling on the process configurations. To illustrate the effect of fouling, scenarios were simulated by varying the fouling rate (parameters a and b in Eq. (14)). The results for the one-stage MD system are given in Figure 10. All operating conditions were kept equal to previous simulations. At low fouling rates both the equipment costs and the utility costs decrease. There is no effect on the cleaning schedule.

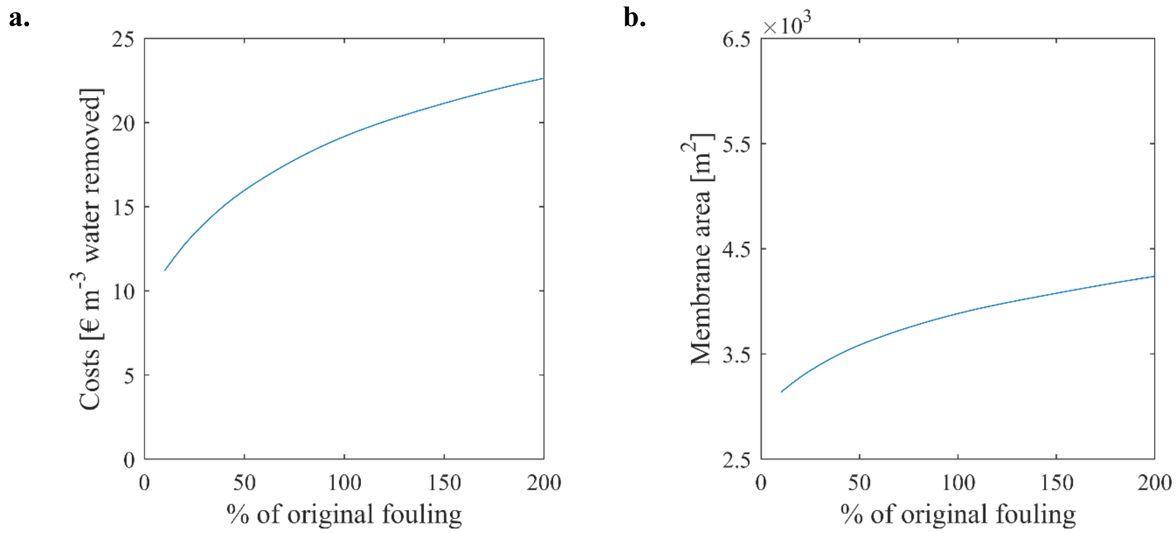

Figure 10. The effect of variation fouling for a one-stage MD system (100% standard fouling, 50% half of fouling rate, 200% doubled fouling rate) on the costs (a) and required membrane area (b).

With flux decline over time, the temperature change of the product in both the hot and the cold side decreases. As a result, the heating and cooling duties, which are the main cost drivers, increase. The heating and cooling duties overshadow the capital related costs. Reduction of the heating and cooling costs by a low fouling rate and keeping high fluxes over time is therefore crucial to make membrane distillation viable.

4.3 Influence of operational conditions and uncertain constants on MD performance

Standard values for operational conditions were used for the discussed optimization of the RO and MD network. These conditions, however, affect the outcomes. Variations of the key operational conditions and membrane properties, like temperature and recirculation settings, give information on the role of the operational conditions for further system improvement.

4.3.1 Effect of operating temperature

Heating and cooling demand are the main cost contributors in MD usage for the concentrating milk. Unlike MD for desalination, where the permeate is the main product [41], cooling is required in the product recirculation. In previous calculations, the temperature of the cold side was set at 10°C and the hot side temperature was set to 58°C. The effect of varying these temperatures on the costs and membrane surface is shown in Figure 11.

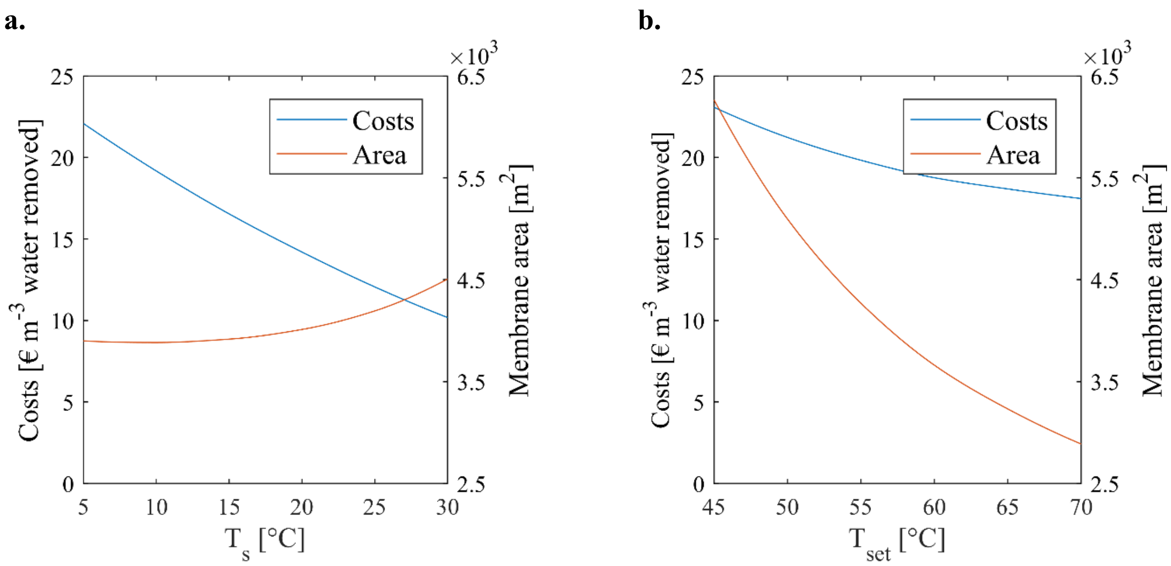

Figure 11. Variation analysis of temperature setpoints for a single-stage MD system. a) Effect of the cold side temperature, T_s, on the processing costs (left axis) and membrane surface (right axis). b) Effect of the hot side temperature, T_{set}, at the processing costs (left axis) and membrane surface (right axis).

Increasing the feed temperature (T_s) from 10 to 20°C reduces the cooling costs. The total membrane surface increases, due to the smaller temperature difference between the hot and cold side. Equipment costs have, compared to the heating and cooling, a small contribution to the costs. The costs decrease by 30% with a change of the feed temperature from 10 to 20°C on the cold side. It should be noted that raising the temperature may increase the risk of microbial contamination.

In previous calculations, the temperature of the hot side (T_{set}) was set to 58°C. Increasing the temperature results in a higher flux and reduces the required membrane area (Figure 11b). As a result, the costs drop due to the higher fluxes and increased heat transfer from the hot to the cold side. The hot side must be as warm as possible, the only limiting factor is the product quality. Temperatures over 60°C for a prolonged time are not desirable for milk due to protein denaturation [43].

4.3.2 Effect of linear flow velocity

The product is recirculated over each module to ensure sufficient crossflow along the membrane. In the system optimization the linear flow velocity was set to 0.05 ms^{-1}. To evaluate the effect on process performance the linear flow velocity was varied between 0.025 and 0.2 ms^{-1}. Increasing the velocity reduces the membrane surface due to higher fluxes (see Figure 12b). The same result was found by Hausmann et al. [10], by showing that higher flow velocities have a positive effect on the flux which results in a smaller membrane surface. An extra advantage of high flow velocities is a lower fouling rate and less flux decline over time. This aspect is also a factor to reduce the required membrane surface. In contrast, Figure 12a gives the effect of varying the linear velocity on the costs, which decrease almost linear towards lower velocities. Lowering the flow velocity also reduces the recirculation rate and consequently the cooling and heating costs. Although also the flux reduces and thus heat transfer from the hot to cold side, the increase in recirculation rate causes a higher energy increase. These calculations do not fully cover the turbulence properties at low velocities. This is a strong assumption, but the results point to the importance of spacer optimisation to reduce the operational costs. Additionally, at higher solids concentrations higher cross flows might be desired, because of the increased viscosity and the shear thinning behaviour of milk [44].

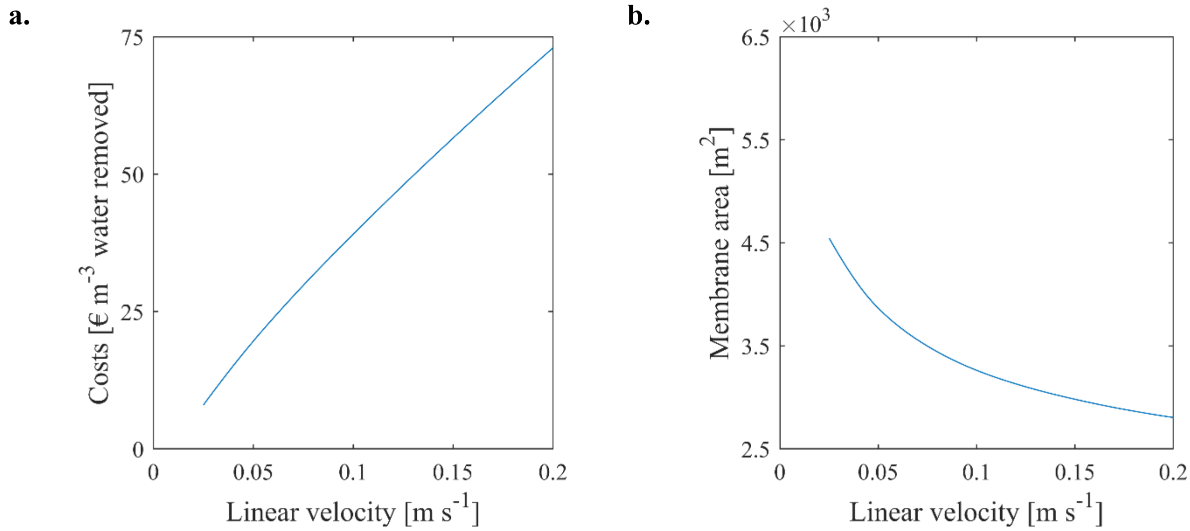

Figure 12. Effect of linear velocity on the costs (a) and required membrane area (b) for a single-stage MD system.

4.4 Use of waste heat

MD operates at a relative low operating temperature and, in contrast to multistage evaporators, MD can make use of low-quality energy streams. In food processing plants low-quality energy streams are often abundantly available [45]. The costs of the high heating demand for MD are reduced by using these low-quality energy streams. Several authors already exploited the potential of membrane distillation in combination with industrial waste heat [17,18,41]. Dow et al. [19] demonstrated the feasibility of operating a MD pilot plant by using waste heat from a gas fired power station. The temperature of the waste heat (less than 40°C was used) had a major influence on the flux of a direct contact membrane distillation unit. Also solar heat has potential as a heat source for membrane distillation [46]. Higher waste heat temperatures result, as expected, in higher fluxes. Figure 11b illustrates the effect of varying set temperature on the required membrane surface and thus capital costs. More important is, however, the reduction of the costs for cooling and heating by using waste heat. Figure 13 gives the operational costs for water removal for different levels waste heat usage, ranging from zero to full replacement of the thermal energy demand by waste heat. Complete energy supply from waste heat, by heat integration with other processes, results in operational costs of 3.1 euro per m^3 water removed. This makes membrane distillation competitive with current concentration techniques. To reach these benefits, additional capital costs are required for waste heat integration. These costs are very case dependent, and will therefore have to be assessed case by case.

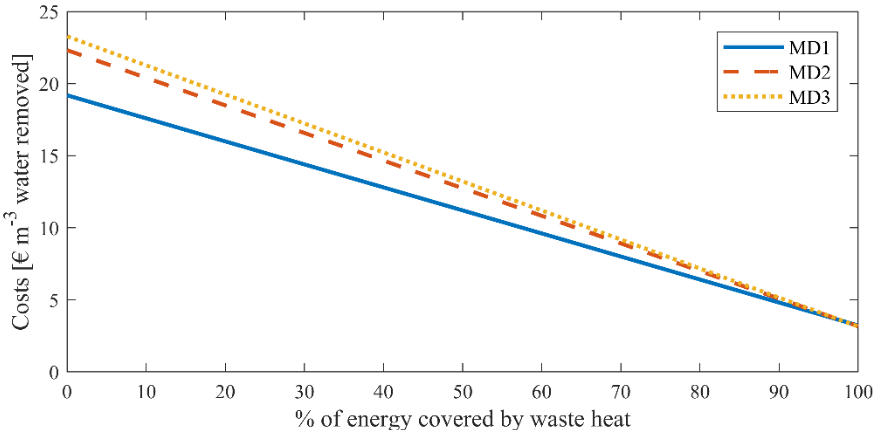

Figure 13. Operational costs as a function of % of required energy for heating and cooling covered by waste heat for MD installations with 1, 2 and 3 stages.

4.5 Membrane distillation system assumptions

Both the configuration of the membrane distillation, and the membrane specifications have influence on the performance. Simulations were based on literature values for physical constants (heat and mass transfer coefficients and condensation layer thickness, see Table 1). In the previous sections the effect of variation of the most important operational conditions (temperature, flow rate, fouling) was discussed. Membrane properties used in this study are based on reported literature or given by a membrane supplier. Experimental work is still required to confirm the findings, and to improve the used values for the membrane properties. The role of the most uncertain constants 1) the thickness of the condensation layer, 2) thickness of the membrane, and 3) thermal conductivity of the membrane were assessed in a sensitivity analysis by ±20% variation of the values given in Table 1. Despite these variations the optimal structure of the MD system was not altered. The most sensitive constant was the thermal conductivity of the membrane with a decrease of 17.6% on the total costs, when the thermal conductivity of the membrane decreases with 20%. The thickness of the condensation layer, and the thickness of the membrane only affects the total costs with 1 – 3%, at ±20% variation.

The membrane resistance was based on Hausmann et al. [10], but changes with the use of different membranes. Halving the membrane resistance (R_m) will increase the flux and reduces both the heating and cooling duties with 18% for a one stage MD system. In order to achieve this advancement, development and testing of new membranes is required. The advantage of internal energy recovery in air gap membrane distillation (AGMD) was the reason to select this MD system for this work. Low fluxes and high recirculation rates proved to limit the internal heat recovery. In this light, direct contact membrane distillation (DCMD) could be a better option. In the AMGD the average temperature difference over the hot side is for the one-stage system 20°C (milk cools down from 58 to 38°C) while the temperature difference over the heater and cooler is 28°C (Figure 6). In this case it is more energy efficient to separate the heating and cooling circuited like in a DCMD. However, if the temperature difference of the hot side is larger compared to temperature difference over the heater, then the AGMD will be beneficial. These results point to the importance for higher fluxes to make the AGMD system viable for milk concentration.

Compared to permeate- or liquid gap membrane distillation (PGMD), the AMGD has a smaller temperature difference as driving force and thus lower flux. According to Swaminathan et al. [47] the PGMD is 20% more energy efficient compared to AGMD. However, due to the liquid on the permeate side there is a higher chance of pore wetting [30], which highly decreases the process performance and thus results in higher costs. Nonetheless, exploring PGMD as option for the concentration of food products is of interest.

5 Conclusion

Membrane distillation (MD) is an emerging technology for product concentration. In this work the potential of different process configurations for the concentration of milk by reverse osmosis (RO) and membrane distillation was assessed and investigated. Although milk was considered as feed, the findings of this work give also important information for application of MD for concentrating of other food products.

Due to the low costs, concentration of milk starts with RO to the maximal possible concentration of milk (18% solids). RO is followed by membrane distillation to concentrate milk to the final 50% solids. The used air gap membrane distillation (AGMD) has the advantage of internal heat recovery and is therefore often preferred over direct contact membrane distillation. Nevertheless, due to the high product recirculation to achieve sufficient cross flow along the membranes the energy costs of the AGMD unit are high. With the current available membranes and energy prices membrane distillation cannot compete with a multi-stage evaporator.

Gradual fouling during the operation has a large influence on process cost of MD, as fluxes decline so does heat transfer. Heating and cooling of product in each stage results in costs that overshadow the costs for membranes and equipment. The optimal configuration of the membrane distillation unit is therefore a single-stage unit that operates at high concentration and low flux. The effect analysis showed the following options for further improvement of the system:1) to increase the cold and hot side temperatures to their maximum acceptable values, 2) to develop spacers that allow lower cross flow velocities in the system and thus lower recirculation rates, and 3) make use of available waste heat.

Acknowledgments

The research leading to these results has received funding from the European Unions's Seventh Framework Programme for research, technological development and demonstration under grant agreement nr. 613732 (ENTHALPY). The authors like to thank partners from the ENTHALPY project, especially L. Feenstra, J. van Medevoort, and J.H. Hanemaaijer (TNO, I3) for their feedback and advice.

Nomenclature

A	Area (m^2)
a, b	Fouling rate parameters
C	Costs (€ yr^{-1})
c	Concentration (kg kg^{-1})
c_p	Specific heat capacity (kJ kg^{-1} K^{-1})
D_w	Membrane water permeability (kg s^{-1} N)
E	Energy requirement (kJ s^{-1})
F	Mass flow (kg s^{-1})
ΔH_v	Latent heat of evaporation (kJ kg^{-1})
h	Heat transfer coefficient (W m^{-2} K^{-1})
J	Water flux (kg m^{-2} s^{-1})
k_f	Mass transfer coefficient (m s^{-1})
k	Thermal conductivity (W m^{-1}K^{-1})
L_f	Lang factor (-)
LF	Equipment life time (year)
M	Number of modules in parallel (-)
N	Number of membrane stages (-)
P	Pressure (Pa)
Q	Heat flow (kJ s^{-1})
R	Mass transfer resistance (Pa m^2 s kg^{-1})
R_{gas}	Universal gas constant (J K^{-1} mol^{-1})

r_{RO}	Fixed recirculation fraction in RO module (-)
T	Temperature (°C)
t	Time (s, h)
v_{lin}	Linear velocity (m s^{-1})
x	Weight fraction (-)

Greek letters

η_{pump}	Energy efficiency of the pump (-)
γ	Variable encompassing the membrane characteristics (-)
δ	Thickness (m)
λ	Conductivity (W m^{-1} K^{-1})
π	Osmotic pressure (Pa)
ρ	Density (kg m^{-3})
ϵ	Constant for the resistance per unit of fouling layer thickness (Pa m s kg^{-1})
ϵ_m	Membrane porosity (-)
μ	Viscosity (Pa s^{-1})

Subscripts

a	Annual
ag	Air gap
b	Bulk
c	Concentrate
cb	Condensing plate – bulk
cl	Condensing layer
cp	Condensing plate
f	Feed
fl	Fouling layer
fm	Fouling – membrane
gm	Air gap – membrane
inv	Investment
m	Mix of feed and recirculated product
mem	Membrane
mod	Membrane module
op	Operational
ov	Overall
p	Permeate
r	Recirculation
s	Cold side variable
set	Hot side variable

References

[1] C. Ramirez, M. Patel, K. Blok, From fluid milk to milk powder: Energy use and energy efficiency in the European dairy industry, Energy. 31 (2006) 1984–2004. doi:10.1016/j.energy.2005.10.014.

[2] P. Walstra, T.J. Geurts, A. Noomen, A. Jellema, M.A.J.S. van Boekel, Dairy Technology : Principles of Milk. Properties and Processes, New York : Marcel Dekker inc., 1999, 1999.

[3] M.S. El-Bourawi, Z. Ding, R. Ma, M. Khayet, A framework for better understanding membrane distillation separation process, J. Memb. Sci. 285 (2006) 4–29. doi:10.1016/j.memsci.2006.08.002.

[4] A. Hausmann, P. Sanciolo, T. Vasiljevic, E. Ponnampalam, N. Quispe-Chavez, M. Weeks, M. Duke, Direct Contact Membrane Distillation of Dairy Process Streams, Membranes (Basel). 1 (2011) 48–58. doi:10.3390/membranes1010048.

[5] V.D. Alves, I.M. Coelhoso, Orange juice concentration by osmotic evaporation and membrane distillation: A comparative study, J. Food Eng. 74 (2006) 125–133. doi:10.1016/j.jfoodeng.2005.02.019.

[6] C.A. Quist-Jensen, F. Macedonio, C. Conidi, A. Cassano, S. Aljlil, O.A. Alharbi, E. Drioli, Direct contact membrane distillation for the concentration of clarified orange juice, J. Food Eng. 187 (2016) 37–43. doi:10.1016/j.jfoodeng.2016.04.021.

[7] S. Nene, S. Kaur, K. Sumod, B. Joshi, K.S.M.S. Raghavarao, Membrane distillation for the concentration of raw cane-sugar syrup and membrane clarified sugarcane juice, Desalination. 147 (2002) 157–160. doi:10.1016/S0011-9164(02)00604-5.

[8] L.D. Tijing, Y.C. Woo, J.-S. Choi, S. Lee, S.-H. Kim, H.K. Shon, Fouling and its control in membrane distillation ─ A review, J. Memb. Sci. 475 (2014) 215–244. doi:10.1016/j.memsci.2014.09.042.

[9] S.N. Moejes, M.J. Romero Guzmán, J.H. Hanemaaijer, K.H. Barrera, L. Feenstra, A.J.B. van Boxtel, Membrane distillation for milk concentration, in: 29th EFFoST Int. Conf. Proc., Athens, Greece, 2015.

[10] A. Hausmann, P. Sanciolo, T. Vasiljevic, U. Kulozik, M. Duke, Performance assessment of membrane distillation for skim milk and whey processing, J. Dairy Sci. 97 (2014) 56–71. doi:10.3168/jds.2013-7044.

[11] E.K. Summers, H.A. Arafat, J.H. Lienhard V, Energy efficiency comparison of single-stage membrane distillation (MD) desalination cycles in different configurations, Desalination. 290 (2012) 54–66. doi:10.1016/j.desal.2012.01.004.

[12] H.C. Duong, P. Cooper, B. Nelemans, T.Y. Cath, L.D. Nghiem, Evaluating energy consumption of air gap membrane distillation for seawater desalination at pilot scale level, Sep. Purif. Technol. 166 (2016) 55–62. doi:10.1016/j.seppur.2016.04.014.

[13] J. Koschikowski, M. Wieghaus, M. Rommel, V.S. Ortin, B.P. Suarez, J.R. Betancort Rodríguez, Experimental investigations on solar driven stand-alone membrane distillation systems for remote areas, Desalination. 248 (2009) 125–131. doi:10.1016/j.desal.2008.05.047.

[14] N. Kuipers, R. van Leerdam, J. van Medevoort, W. van Tongeren, B. Verhasselt, L. Verelst, M. Vermeersch, D. Corbisier, Techno-economic assessment of boiler feed water production by membrane distillation with reuse of thermal waste energy from cooling water, Desalin. Water Treat. 3994 (2014) 1–13. doi:10.1080/19443994.2014.946722.

[15] L. Mar Camacho, L. Dumée, J. Zhang, J. Li, M. Duke, J. Gomez, S. Gray, L.M. Camacho, L. Dumée, J. Zhang, J. De Li, M. Duke, J. Gomez, S. Gray, Advances in membrane distillation for water desalination and purification applications, Water. 5 (2013) 94–196. doi:10.3390/w5010094.

[16] D. González, J. Amigo, F. Suárez, Membrane distillation: Perspectives for sustainable and improved desalination, Renew. Sustain. Energy Rev. 80 (2017) 238–259. doi:10.1016/j.rser.2017.05.078.

[17] A. Hausmann, P. Sanciolo, T. Vasiljevic, M. Weeks, M. Duke, Integration of membrane distillation into heat paths of industrial processes, Chem. Eng. J. 211–212 (2012) 378–387. doi:10.1016/j.cej.2012.09.092.

[18] N.A. Elsayed, M.A. Barrufet, M.M. El-Halwagi, Integration of Thermal Membrane Distillation Networks with Processing Facilities, Ind. Eng. Chem. Res. 53 (2014) 5284–5298. doi:10.1021/ie402315z.

[19] N. Dow, S. Gray, J. Li, J. Zhang, E. Ostarcevic, A. Liubinas, P. Atherton, G. Roeszler, A. Gibbs, M. Duke, Pilot trial of membrane distillation driven by low grade waste heat: Membrane fouling and energy assessment, Desalination. 391 (2016) 30–42. doi:10.1016/j.desal.2016.01.023.

[20] S.Y. Alnouri, P. Linke, A systematic approach to optimal membrane network synthesis for seawater desalination, J. Memb. Sci. 417–418 (2012) 96–112. doi:10.1016/j.memsci.2012.06.017.

[21] C.S. Khor, B. Chachuat, N. Shah, A superstructure optimization approach for water network synthesis with membrane separation-based regenerators, Comput. Chem. Eng. 42 (2012) 48–63. doi:10.1016/j.compchemeng.2012.02.020.

[22] M. Zhu, Optimal design and scheduling of flexible reverse osmosis networks, J. Memb. Sci. 129 (1997) 161–174. doi:10.1016/S0376-7388(96)00310-9.

[23] M.M. El-Halwagi, Synthesis of reverse-osmosis networks for waste reduction, AIChE J. 38 (1992) 1185–1198. doi:10.1002/aic.690380806.

[24] B.K. Srinivas, M.M. El-Halwagi, Optimal design of pervaporation systems for waste reduction, Comput. Chem. Eng. 17 (1993) 957–970. doi:10.1016/0098-1354(93)80077-Z.

[25] R. González-Bravo, F. Nápoles-Rivera, J.M. Ponce-Ortega, M. Nyapathi, N. Elsayed, M.M. El-Halwagi, Synthesis of optimal thermal membrane distillation networks, AIChE J. 61 (2015) 448–463. doi:10.1002/aic.14652.

[26] A. Hausmann, P. Sanciolo, T. Vasiljevic, M. Weeks, K. Schroën, S. Gray, M. Duke, Fouling mechanisms of dairy streams during membrane distillation, J. Memb. Sci. 441 (2013) 102–111. doi:10.1016/j.memsci.2013.03.043.

[27] M. Ramezanianpour, M. Sivakumar, An analytical flux decline model for membrane distillation, Desalination. 345 (2014) 1–12. doi:10.1016/j.desal.2014.04.006.

[28] N.M. D'Souza, A.J. Mawson, Membrane Cleaning in the Dairy Industry: A Review, Crit. Rev. Food Sci. Nutr. 45 (2005) 125–134. doi:10.1080/10408690490911783.

[29] A. Hausmann, P. Sanciolo, T. Vasiljevic, M. Weeks, K. Schroën, S. Gray, M. Duke, Fouling of dairy components on hydrophobic polytetrafluoroethylene (PTFE) membranes for membrane distillation, J. Memb. Sci. 442 (2013) 149–159. doi:10.1016/j.memsci.2013.03.057.

[30] E. Drioli, A. Ali, F. Macedonio, Membrane distillation: Recent developments and perspectives, Desalination. 356 (2015) 56–84. doi:10.1016/j.desal.2014.10.028.

[31] F. Fernández-Martín, Influence of temperature and composition on some physical properties of milk and milk concentrates. II. Viscosity, J. Dairy Res. 39 (1972) 75. doi:10.1017/S0022029900013868.

[32] Y. Choi, M.R. Okos, Effects of Temperature and Composition on the Thermal Properties of Foods, Food Eng. Process Appl. (1986) 93–101.

[33] R. Field, Fundamentals of Fouling, in: Membr. Technol., Wiley-VCH Verlag GmbH & Co. KGaA, Weinheim, Germany, 2010: pp. 1–23. doi:10.1002/9783527631407.ch1.

[34] A.J.B. van Boxtel, Strategies for Optimal Control of Membrane Fouling: Reverse Osmosis of Cheese Whey, a Case Study, Netherlands Institute for Dairy Research (NIZO), 1991.

[35] A.J.B. van Boxtel, Z.E.H. Otten, H.J.L.J. van der Linden, Evaluation of process models for fouling control of reverse osmosis of cheese whey, J. Memb. Sci. 58 (1991) 89–111. doi:10.1016/S0376-7388(00)80639-0.

[36] F. Evangelista, A short cut method for the design of reverse osmosis desalination plants, Ind. Eng. Chem. Process Des. Dev. 24 (1985) 211–223. doi:10.1021/i200028a036.

[37] C. Duclos-Orsello, W. Li, C.-C. Ho, A three mechanism model to describe fouling of microfiltration membranes, J. Memb. Sci. 280 (2006) 856–866. doi:10.1016/j.memsci.2006.03.005.

[38] R.H. Perry, D.W. Green, Perry's Chemical Engineers' Handbook, Seventh Ed, McGraw-Hill, 1997.

[39] Y. Muramatsu, A. Tagawa, T. Kasai, Effective Thermal Conductivity of Rice Flour and Whole and Skim Milk Powder, J. Food Sci. 70 (2006) E279–E287. doi:10.1111/j.1365-2621.2005.tb07184.x.

[40] Y. Lu, Y. Hu, D. Xu, L. Wu, Optimum design of reverse osmosis seawater desalination system considering membrane cleaning and replacing, J. Memb. Sci. 282 (2006) 7–13. doi:10.1016/j.memsci.2006.04.019.

[41] G.W. Meindersma, C.M. Guijt, A.B. de Haan, Desalination and water recycling by air gap membrane distillation, Desalination. 187 (2006) 291–301. doi:10.1016/j.desal.2005.04.088.

[42] H.J. See, V.S. Vassiliadis, D.I. Wilson, Optimisation of membrane regeneration scheduling in reverse osmosis networks for seawater desalination, Desalination. 125 (1999) 37–54. doi:10.1016/S0011-9164(99)00122-8.

[43] J.N. de Wit, G. Klarenbeek, Effects of Various Heat Treatments on Structure and Solubility of Whey Proteins, J. Dairy Sci. 67 (1984) 2701–2710. doi:10.3168/jds.S0022-0302(84)81628-8.

[44] K.R. Morison, J.P. Phelan, C.G. Bloore, Viscosity and Non-Newtonian Behaviour of Concentrated Milk and Cream, Int. J. Food Prop. 16 (2013) 882–894. doi:10.1080/10942912.2011.573113.

[45] M. Papapetrou, G. Kosmadakis, A. Cipollina, U. La Commare, G. Micale, Industrial waste heat: Estimation of the technically available resource in the EU per industrial sector, temperature level and country, Appl. Therm. Eng. 138 (2018) 207–216. doi:10.1016/j.applthermaleng.2018.04.043.

[46] H. Chang, G.-B. Wang, Y.-H. Chen, C.-C. Li, C.-L. Chang, Modeling and optimization of a solar driven membrane distillation desalination system, Renew. Energy. 35 (2010) 2714–2722. doi:10.1016/j.renene.2010.04.020.

[47] J. Swaminathan, H.W. Chung, D.M. Warsinger, F.A. AlMarzooqi, H.A. Arafat, J.H. Lienhard V, Energy efficiency of permeate gap and novel conductive gap membrane distillation, J. Memb. Sci. 502 (2016) 171–178. doi:10.1016/j.memsci.2015.12.017.

Appendix

A.1 Process data

Table A.1 Operating and optimization conditions for both RO and MD process.

Parameter	RO	MD
Starting temperature feed (°C)	10	10
Temperature permeate (°C)	10	-
Pressure feed (Pa)	40×10^5	10^5
Pressure drop over the module (Pa)	0.22×10^5	0.2×10^5
Pressure permeate (Pa)	10^5	-
Starting pressure feed (Pa)	10^5	-
Feed flow (kg h^{-1})	25000	25000 – 12500
Starting concentration (w/w)	0.09	≤ 0.18
Final concentration (w/w)	≤ 0.18	0.50
Linear velocity (m s^{-1})	2	0.049
Annual operating time (h)	8000	8000
Cleaning cycle time (h)	1	1
Operating cycle time (h)	7	7
Number of stages, N (-)	1 – 5	1 – 5
Equipment life time (year)	15	15
Membrane life time (year)	4	4

Table A.2 Economic data (based on [22,25,40]).

Parameter	Value
Investment cost pump (€)	$2590(P_{pump})^{0.79}$
Pump efficiency	0.85
Investment cost heater/cooler (€)	$1115F_{tot}$
Lang factor	1.4
Equipment lifetime (y)	15
MD module costs (€ m^{-2})	58.5
MD membrane costs (€ m^{-2})	100
RO module costs (€ m^{-2})	58.5
RO membrane costs (€ m^{-2})	17.75
Heating costs (€ GJ^{-1})	4.0
Cooling costs (€ GJ^{-1})	3.0
Electrical costs (€ kWh^{-1})	0.12
Cleaning cost (€ m^{-2} $hour^{-1}$)	0.017

A.2 MD fouling model validation

In order to include fouling in the MD model, an estimate for the fouling resistance was made. Figure A.1 shows the fitting of the lumped parameters a and b for the estimation of the fouling resistance (R_f) as given in Eq. (14). Data from Hausmann et al [10] was used the estimate the lumped parameters a and b. Initial fouling build up is well fitted as can be seen in the comparison between the simulation and the data in the figure below. When the fouling layer build up stabilises (roughly after 8 hours) the flux is underestimated for low concentrations (20%) and overestimated at high concentrations (40%).

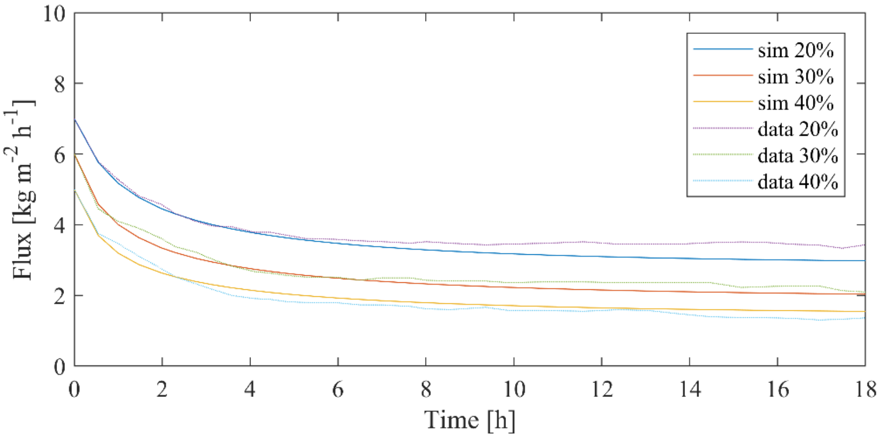

Figure A.1. Result of the fitting of the flux at different concentrations 20, 30 and 40% dry matter. The dotted lines are the actual data (data) [10] **and the solid lines are the fitted simulations (sim).**

The resistance over the air gap is based on the molecular diffusion model [30]:

$$R_{ag} = \left(\frac{\epsilon D P_t}{\delta_{ag} P_{ag,log}} \frac{M_v}{R(T_{ag,avg} + 273.15)} \right)^{-1} \quad (A.1)$$

where $T_{ag,avg}$ is the mean temperature in the air gap, $P_{ag,log}$ is the log mean pressure in the gap, P_t is the total pressure, ϵ is the membrane porosity, M_v the molar mass of water molecules, D is the water vapour diffusion coefficient through air.

A.3 Alternative MD configurations

In this section the results are presented for the other membrane distillation configurations.

Table A. 3. Results for other MD configurations with 2, 3, 4, or 5 stages in series.

		MD 2	**MD 3**	**MD 4**	**MD 5**
Feed	tonne h^{-1}	12.5	12.5	12.5	12.5
Total membrane area	m^2	3448	3340	3329	3299
Number of stages	-	2	3	4	5
Number of parallel units in subsequent stages	-	3-3	3-3-3	3-3-3-3	3-3-3-3-3
Heating costs	€ m^{-3}	10.3	10.9	10.9	10.8
Cooling costs	€ m^{-3}	7.2	7.5	7.3	7.1
Electrical costs	€ m^{-3}	2.0	2.2	2.2	2.3
Equipment costs	€ m^{-3}	1.9	1.9	1.9	1.9
Cleaning costs	€ m^{-3}	0.9	0.9	0.9	0.9
Total costs	€ m^{-3}	22.3	23.3	23.2	23.0

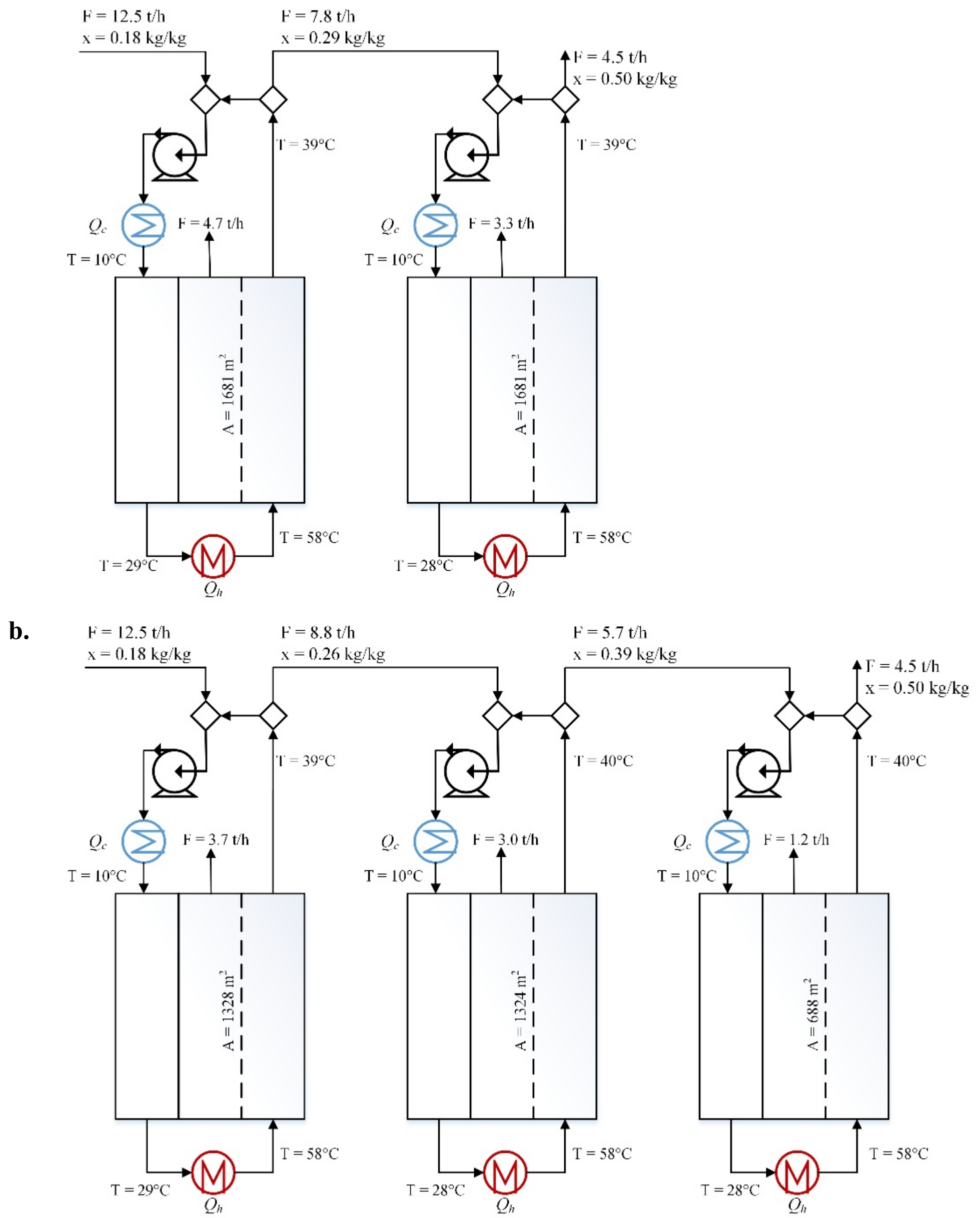

Figure A.2. Optimal process configurations for the MD configuration with 2 (a) and 3 (b) stages, including average flows, concentrations, and temperatures.